ENGINE – **EN**hanced **G**eothermal **I**nnovative **N**etwork for **E**urope
Workshop 3, "Stimulation of reservoir and microseismicity"
Kartause Ittingen, Zürich, June 29 – July 1, 2006, Switzerland

Detection of flow pathway structure upon pore pressure distribution estimated from hydraulically induced microseismic events and application to the Soultz HDR field

Takatoshi ITO
Institute of Fluid Science, Tohoku University
2-1-1 Katahira, Aoba-ku
Sendai, Miyagi, 980-8577, Japan
e-mail: ito@ifs.tohoku.ac.jp

Abstract

In the hydraulic stimulation, massive fluid is injected into subsurface rock through drilled wells. Then a number of microseismic events are commonly observed. By analyzing those data of microseismic events, we can estimate the orientation, i.e. dip and strike, of the fracture which slides to induce microseismic event. From the estimated fracture orientation, taking into account the in situ stresses and the Mohr-coulomb criterion to describe the critical condition of fracture sliding, we can estimate the pore pressure at the location of sliding fracture and at the time when the sliding occurs, in other words, when the microseismic event occurs. The estimated values of pore pressure are sorted in a certain manner for each equally divided spatial region, i.e. block or cell, to give spatial distribution of pore pressure and its variation with time during hydraulic stimulation. Furthermore, we have shown that the location of flow pathways and the hydraulic conductivity along them could be estimated from the pore pressure distribution estimated from microseismic events.

Keywords: stimulation, microseismic event, pressure propagation, flow pathway

1. Introduction

Fracture networks are used for underground heat exchangers, i.e. reservoirs, in the Enhanced Geothermal Systems (EGS). Each fracture composed of the network is spread over a relatively large area of several hundreds square meters, but its aperture is limited to several millimeters at maximum. There is no way to detect directly such a thin structure nor the fluid flow in it from ground surface through a huge rock mass with few thousands meters in thickness, while those factors are important for construction of the EGS. On the other hand, a number of microseismic events are observed during hydraulic stimulation. It is believed that the occurrence of those events is associated with the fluid flow through fracture networks caused by the stimulation. Therefore it may be possible to estimate the fluid flow from the observed micoseismic events. To this end, we have considered the sequence in which hydraulic stimulation leads to the occurrence of microseismic events. Then, based on those consideration, we have come up with an idea to integrate the data of microseismic events for estimating pore pressure propagation along the fracture network associated with hydraulic stimulation (Ito et al., 2004, Osada et al., 2005, Ito et al., 2006). Furthermore, we have shown that the location of flow pathways and the hydraulic conductivity along them could be estimated from the pore pressure distribution estimated from microseismic events. To do this, we assume an appropriate model of flow pathway structure and adjust it as the pore pressure distribution computed by the model agrees well with that estimated from micro-seismic events (Ito et al., 2004). In this paper, those concepts and procedure which have been proposed in our previous works, will be summarized, and the outline of the analyses in which we have applied the proposed method to the Soultz HDR site in France will be presented.

2. Concept and procedure

2.1 Estimation of pressure distribution

Microseismic events are considered to be occurred by the following sequence; hydraulic stimulation drives pressure propagation through fracture network, then the pore pressure in pre-existing fractures is increased, the additional pressure affects to reduce friction between the fracture planes, as a result, shear slipping occurs on the fractures, and finally the slipping generates elastic waves to be observed as the microseismic events.

Friction between fracture planes is given by $\mu(S_n - P_p)$, where μ is the coefficient of friction along the fracture plane, S_n is the normal stress of fracture and P_p is pore pressure in the fracture (**Fig. 1**). The friction decreases

with increasing P_p until P_p reaches the critical pore pressure P_c at which the friction decreases to be balanced with the shear stress of fracture, τ, and then shear slipping occurs on the fracture. Such a critical condition is well known as the Coulomb criterion, and is given by

$$|\tau| = \mu(S_n - P_c) \quad (1)$$

The stress components S_n and τ are given as functions of the fracture orientation and the regional state of stress as follows;

$$\tau = \left\{\lambda_1^2\lambda_2^2(S_1 - S_2)^2 + \lambda_2^2\lambda_3^2(S_2 - S_3)^2 + \lambda_3^2\lambda_1^2(S_3 - S_1)^2\right\}^{\frac{1}{2}} \quad (2)$$

$$S_n = \lambda_1^2 S_1 + \lambda_2^2 S_2 + \lambda_3^2 S_3 \quad (3)$$

where S_i (i = 1, 2, 3, $S_1 > S_2 > S_3$) are principal components of the regional stresses, and λ_i (i = 1, 2, 3) are direction cosines between normal to the fracture plane and the axes of S_1, S_2 and S_3 respectively.

On the other hand, the detailed analysis of the microseismic events allows us to detect not only the seismic location but also the dip and strike of the fracture on which shear slipping occurs to cause the microseismic events. Thus if the principal stresses S_i and those orientations are given in another way, the direction cosines λ_i can be determined from the analysis of the microseismic events. In this case, the stresses S_n and τ are to be known from Eqs. (2) and (3), and therefore, the value of P_c can be estimated so as to satisfy Eq. (1) assuming an appropriate value of μ e.g. $\mu = 0.8$. This fact implies that we can estimate the value of pore pressure at the location and time of each microseismic event. This idea has been originally proposed by Cornet and Yin (1995), and recently we have proposed an idea how to integrate the estimated value of P_c for each microseismic event into a spatial distribution of pore pressure induced by hydraulic stimulation (Ito et al., 2004, Osada et al., 2005). To do this, we have introduced the concept of 'block' (or 'cell' in other words). We divide the region of interest into square blocks with the same size as schematically shown in **Fig. 2 (a)**, and we assume that the microseismic events involved in each one of the blocks are induced by the elevated pore pressure brought by a flow pathway passing through the block. When the estimated values of P_c of the microseismic events involved in a block are plotted on the pressure - time diagram, the results may be as illustrated by cross marks in **Fig. 2(b)**. The values of P_c should be equal to or lower than the pore pressure P in the flow pathway

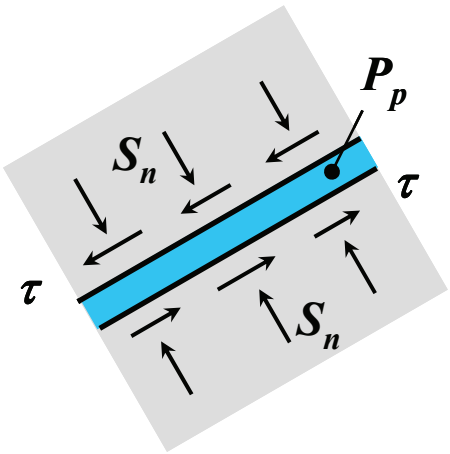

Figure. 1. Fracture subjected to stress and pressure.

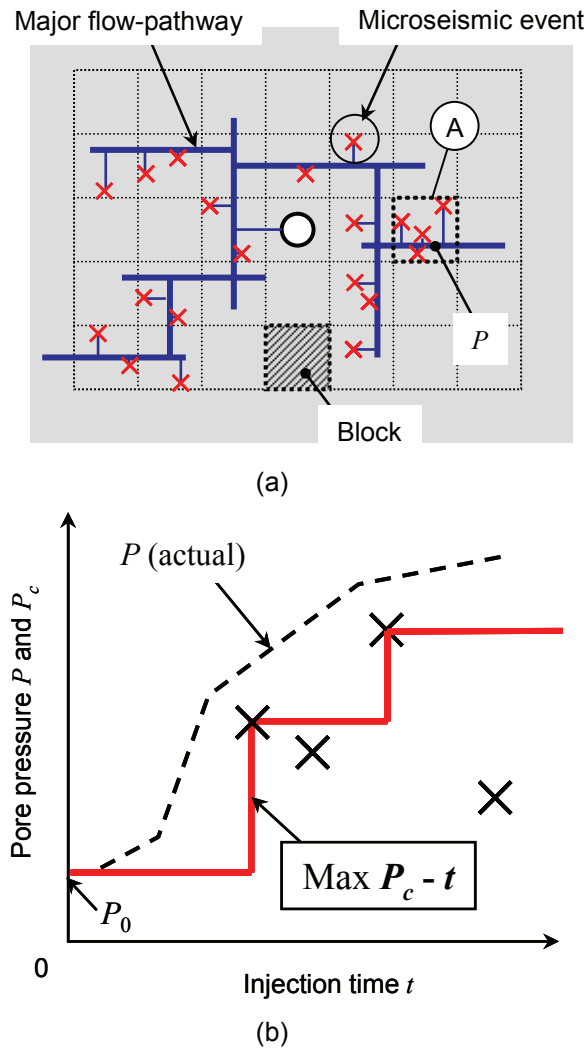

Figure. 2. (a) Concept of 'block', and (b) the relationship between the pore pressure P in the flow pathway and the critical pore pressure Pc estimated from each one of microseismic events involved in the block 'A' shown in A.

passing through the block. It is hard to predict specifically the relationship between P and P_c, which should be a function of unknown factors such as hydraulic conductivity in the branches connecting the pathway and the fractures in principle. However, it is reasonable to consider that microseismic events associated with larger P_c should occur according to an increase in P. Therefore, when we collect the maximum value of P_c in the past at each time, its variation with time such as the solid line in Fig. 2(b), should have a similar tendency with the actual variation of P such as the dashed line in Fig. 2(b). In this reason, we assume that the dashed line, i.e. the variation of P with time, could be estimated approximately as the solid line in each one of the blocks, and by compiling those results, the regional pressure distribution could be estimated finally. Hereafter we will refer to the relationship shown by the solid line in Fig. 2(b) as the maximum $P_c - t$ relationship for simplicity. The more detailed discussion with this concept is referred to Ito et al. (2004) and Osada et al. (2005).

2.2 *Estimation of flow pathways*

On the other hand, pore pressure distribution should change according to location of flow-pathways and distribution of hydraulic conductivity along them. Therefore, we could estimate flow-pathway structure as it gives a good explanation of the pore pressure distribution estimated from microseismic events. To this end, we assume an appropriate model of flow-pathway structure and adjust it as the pore pressure distribution computed by the model agrees well with that estimated from microseismic events.

Fig. 3(a) illustrates a model of flow-pathway structure for a 2D case. Again we divide the region in concern into square blocks as they are consistent with the blocks used for the estimation of pore pressure distribution from microseismic events (see Fig. 2(a)). We assume hydraulic conductivity between the adjacent blocks, and the conductivity is modeled by a slit-like flow-pathway (**Fig. 3(b)**) which is hereafter referred to the pathway-unit. The pathway-unit is assumed to be located connecting each center of the adjacent blocks, and it has a constant width w everywhere but its height H varies one by one according to the degree of local hydraulic conductivity. There is additional fluid storage connecting with the pathway-unit, which represents fluid volume in the fractures whose one side is open to flow-pathway but the opposite side is closed, and so fluid flow is not expected through them. The storage volume is defined per unit length of the pathway-unit, and is denoted by v_s. This parameter is of course independent of

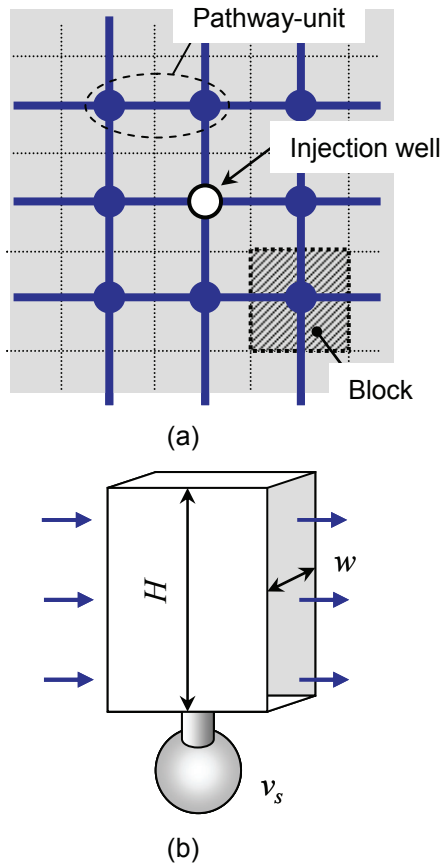

Figure. 3. (a) A 2D model of flow pathway, and (b) structure of the pathway-unit shown in Fig. (a).

hydraulic conductivity, but it is necessary, since such a kind of fluid volume controls the mean velocity of pressure propagation. In the present study, the volume is assumed constant everywhere.

3. Application to the Soulz HDR site

3.1 *Pressure distribution*

The Soultz project began in 1989 when well GPK1 was drilled to 2000 m, penetrating 400 m into the crystalline granite basement of the Rhine graben. In 1992, the well was extended to a total depth of 3600 m and the casing shoe set at 2850 m, leaving some 750 m open hole. In September, 1993, a major hydraulic stimulation test which is to be the object of the present study, was carried out, and then fresh water was injected into the rock formation through the open hole section of well GPK-1 for a period of 17 days. There are microseismic events of 12,837 in total, whose locations were successfully detected (Jones et al., 1995). We examined the focal mechanism using the P-wave first motion data of those events, and then for a subset of 2,285 events, we succeeded in finding the fault plane solutions as the orientation of fractures on

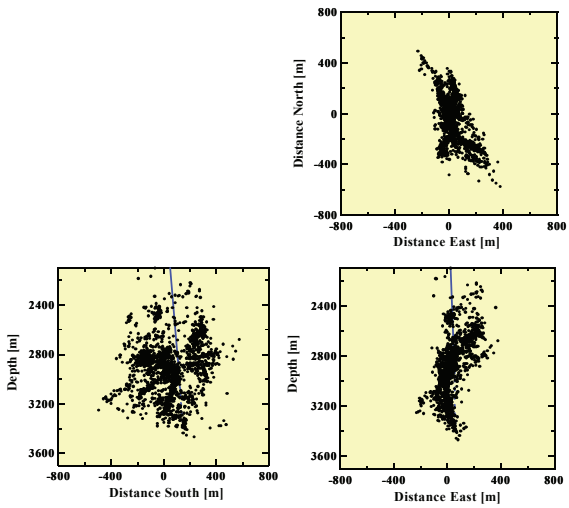

Figure. 4. Location of microseismic events observed during the stimulation of GPK-1 in 1993.

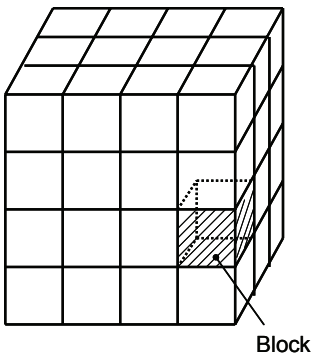

(a)

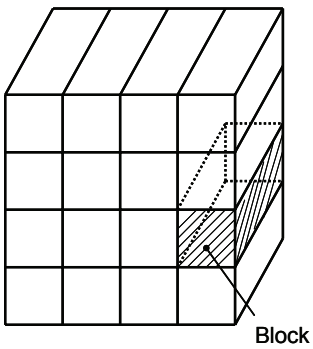

(b)

Figure. 5. Division into the blocks with the shape of (a) cubic and (b) rectangular parallel piped.

which shear sliding occurred to cause the microseismic events (**Fig. 4**). For each one of the fractures whose orientations were determined as the focal plane solution, the critical pore pressure required for the fracture to slide, P_c, was evaluated.

The shape and size of the blocks for the estimation of pore pressure distribution are basically arbitrary as long as they are the

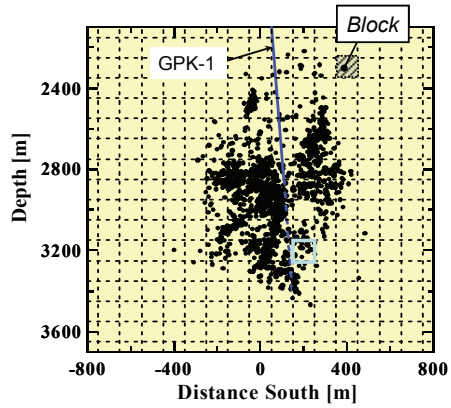

(a)

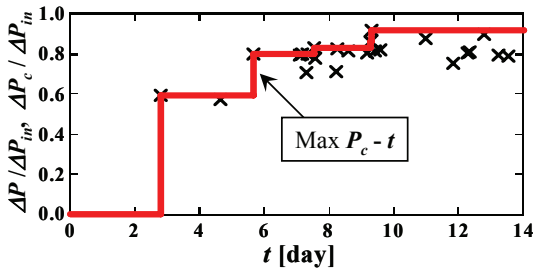

(b)

Figure. 6. (a) Division of the blocks, and (b) estimated pore pressure variation in the block located at the horizontal and vertical positions of "Distance south"=200 m and "Depth" = 3200 m in Fig. (a).

same everywhere (**Fig. 5**). For this analysis we assumed here two-dimensional division of the blocks for simplification so that the block is set to be a rectangular parallelepiped as schematically shown in Fig. 5(b). Taking into account the fact that the microseismic events distributed in the region which is wide in the N-S direction but thin in the E-W direction as can be seen from Fig. 4, the blocks are set to be oriented so that their long side is aligned in the E-W direction. The cross section of the block is 100 x 100 m^2, and the length of the block is such that each one of the microseismic events is involved in one of the blocks. On these arrangements, we estimated the pore pressure variation with time for each one of the blocks. **Fig. 6** shows an example. In the figures, we plotted (ΔP_c /ΔP_{in}) and (ΔP /ΔP_{in}) in ordinate and the elapsed time t in abscissa, where the ΔP_c and ΔP denote (P_c - P_0) and (P - P_0) respectively and P_0 is the initial value of pore pressure, ΔP_{in} denotes (P_{in} - P_{in0}), P_{in} is the well-head pressure at the injection well and P_{in0} is the well-head pressure before the injection is started. The value of ΔP_{in} is here set to be 9 MPa. The cross marks represent the estimated values of the critical pore pressure, P_c, to cause the microseismic events

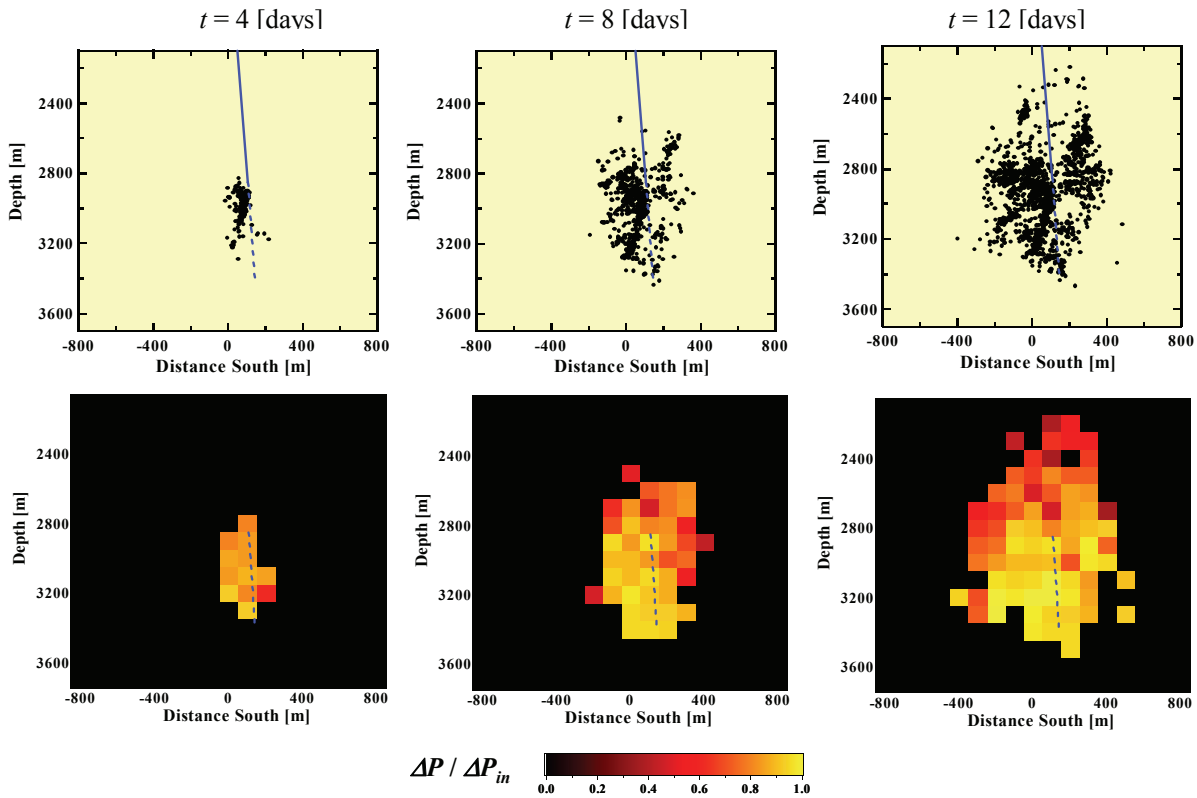

Figure 7. (Top) Locations of microseismic events which occurred until the indicated time, and (bottom) pore pressure distribution estimated from those microseismic events.

involved in the block, and the solid lines represent the P_c-t relationship which is obtained by connecting the maximum value of P_c in the past at each time. The maximum P_c -t relationship should represent approximately the variation of the pore pressure inside the flow pathway at the location of the block. In the same way, we estimated the maximum P_c -t relationship for each one of the blocks where the microseismic events are involved. The results are summarized in the set of figures at the lower side of **Fig. 7**, where those figures show the spatial distribution of the estimated pore pressure at the selected time of t = 4, 8 and 12 [days]. The set of figures at the upper side of Fig. 7, show the locations of microseismic events which occurred until each one of the selected times. The dashed lines denote the open hole section of the injection well. From those results, we can see that relatively high pressure was induced in the blocks including the open hole section of the injection well. The high pressure propagated into the surrounding region gradually with time, and then there appeared a pressure gradient in the outward direction from the location of the open hole section. Such a tendency is reasonable, since the injected fluid flowed out from the open hole section into the surrounding rock formation. The pressure gradient in the upward direction appeared more clearly in the results. It should be noted here that the gradient did not arise from hydrostatic pressure gradient with depth, since we used here the index of ΔP for representing pressure distribution and the ΔP denotes the increment of pore pressure from its initial value, i.e. hydrostatic pressure.

3.2 *Flow pathway structure*

We assumed the 2D model of flow pathway structure as shown in Fig. 3(a), and optimized the height H and the storage volume v_s of the model as the pore pressure distribution computed by the model agrees well with the pore pressure distribution estimated from microseismic events. In order for simplification, it was assumed that H depends on the location but v_s is uniform everywhere. For the model optimization, we used the pore pressure distribution at t = 4, 8 and 12 [days] shown in Fig. 7 and also the pore pressure distribution at t = 5, 7 and 10 [days] estimated from the microseismic events in the same way to obtain Fig. 7. Note that by using the pore pressure distribution not only at a certain time but several different times, we can optimize a lot of unknowns of H and v_s with more accuracy.

Fig. 8(a) shows the distribution of H which was obtained finally by the model optimization. The blue color shows a region in which the microseismic events were observed, in other words, the pore pressure distribution was estimated. As can be seen easily, the flow pathway structure can be estimated for that region basically. Each tick mark in the figure

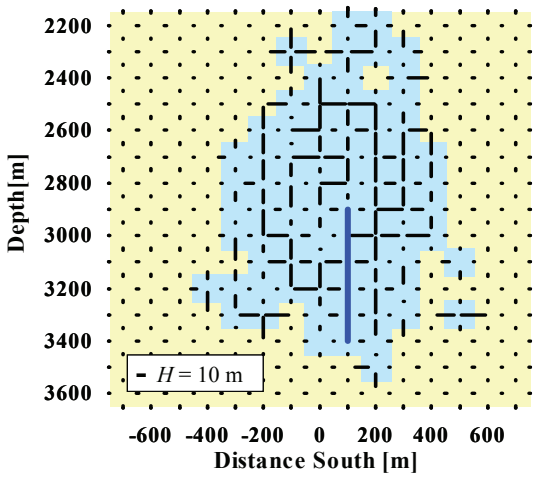

(a)

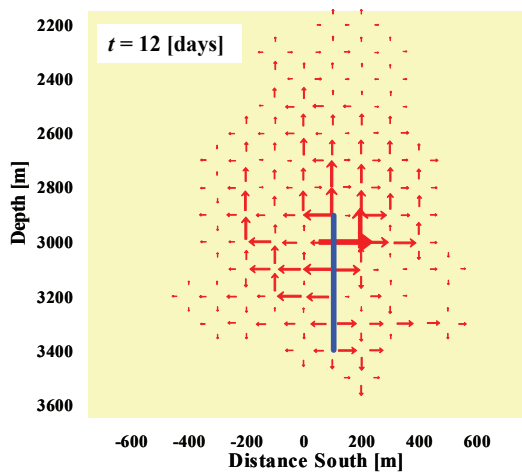

(b)

Figure. 8. (a) Estimated flow pathway, and (b) simulated flow distribution assuming the 1993 stimulation.

denotes the location of the assumed slit-like flow pathway, where its length is proportional to the height of flow pathway, H. The storage vole v_s was estimated to be 400 m^3/m. A thick blue line denotes the open hole section of the injection well, i.e. GPK-1. The result shows that conductive flow pathways are aligned in vertical direction rather than the horizontal direction. On the other hand, if the flow pathway could be detected, in principle we could estimate fluid flow through the flow pathways at arbitral conditions. Thus **Fig. 8(b)** shows the estimated distribution of fluid flow through the flow pathways of Fig. 8(a) assuming that GPK-1 is pressurized at the condition of ΔP_{in} = 9 MPa as same as the hydraulic stimulation in 1993, where the arrow in red shows the flow direction and its length is proportional to the flow rate. This figure shows that the large amount of fluid enters the rock mass from the upper part of the open hole section of GPK-1. This result is consistent with the fact recorded in flow logs that some 60 % of the injected fluid entered the rock mass at the upper zone of the open hole section (Jones et al., 1995, Evans et al., 2005). The entering fluid tends to flow upward in accordance with the anisotropy of higher conductivity in vertical direction.

4. Conclusions

We presented here a method to estimate the pressure propagation in reservoirs during hydraulic stimulation by using the data of microseismic events. The estimated pressure distribution allows us to infer the fluid flow in reservoirs caused by the hydraulic stimulation. Furthermore, by using the estimated pressure distribution, we can estimate quantitatively the spatial distribution of hydraulic conductivity in reservoirs. To do this, we assume an appropriate model of flow pathway structure and optimize it as the pore pressure distribution computed by the model agrees well with that estimated from microseismic events. Thus if the flow pathways can be detected accurately, based upon the results, we can carry out case studies such as estimating the best arrangement of injection and production wells, the recovery rate and the flow impedance etc. The achievement of this kind of techniques should improve drastically the procedure to design and control the HDR systems, and it should bring a big thrust to drive the HDR development.

5. Acknowledgement

We would like to acknowledge the members of the MURPHY/MTC International Collaborative Projects for their support and encouragement.

6. References

Cornet, F.H. and Yin, J. (1995), “Analysis of Seismicity for Stress Field Determination and Pore Pressure Mapping,” *Pure Appl. Geophys.*, **145**, 677-700.

Evans, K.F., Genter, A. and Sausse, J. (2005), “Permeability Creation and Damage due to Massive Fluid Injections into Granite at 3.5 km at Soultz,” *J. Geophys. Res.*, **110**, B04203.

Ito, T., Osada, K. and Hayashi, K. (2004), “Detection of Flow-pathway Structure upon Pore-pressure Distribution Estimated from Hydraulically-induced Micro-seismicity,” *Proc. the 6th North American Rock Mech. Symp. (NARMS)*, Houston, ARMA/NARMS 04-602 (CD-ROM).

Ito, T., Chiba, T., Osada, K. and Hideshi, K. (2006), “A New Approach for Monitoring Pressure Propagation in Reservoirs Based on Microseismic Events Caused by Hydraulic Stimulation,” *Proc. the 31st Workshop Geother.*

Reservoir Eng., Stanford, pp.372-377 (CD-ROM).

Jones, R. H., Beauce, A., Jupe, A., Fabriol, H. and Dyer, B.C. (1995), "Imaging induced microseismicity during the 1993 injection tests at Soultz-sous-Forêts, France," *Proc. World Geother. Cong.*, Florence, pp. 2,665-2,669.

Osada, K., Ito, T., Hayashi, K. and Baria, R. (2005), "Mapping of Propagating Pressure in Reservoir from the Data of Microseismic Events in the 1993 Hydraulic Stimulation at the Soultz HDR Site," *Geother. Resour. Coun. Trans.*, **29**, 109-114.